Molecular dynamics calculations of the crystal-melt interfacial mobility for hexagonal close-packed Mg

Z. G. Xia,[1] D. Y. Sun,[1] M. Asta,[2] and J. J. Hoyt[3]
[1]*Key Laboratory of Optical and Magnetic Resonance Spectroscopy and Department of Physics, East China Normal University, Shanghai 200062, China*
[2]*Department of Chemical Engineering and Materials Science, University of California at Davis, Davis, California 95616, USA*
[3]*Sandia National Laboratories, Albuquerque, New Mexico 87185, USA*
(Received 31 August 2006; published 8 January 2007)

The kinetics of crystallization from the melt is investigated for hcp Mg employing molecular dynamics simulations based on a recently developed embedded-atom-method interatomic potential. The interface mobility (μ), defined as the constant of proportionality between interface velocity and undercooling, is calculated for the three high-symmetry orientations (0001), $(10\bar{1}0)$, and $(11\bar{2}0)$. The magnitudes of the interface mobilities are found to lie in the range of 40–80 cm/s/K. The mobilities $\mu_{10\bar{1}0}$ and $\mu_{11\bar{2}0}$ are found to be of comparable magnitude and approximately 1.7 times larger than μ_{0001}. The calculated dependence of μ on interface normal is discussed within the framework of the kinetic density-functional theory (DFT) formulation of Mikheev and Chernov.

DOI: 10.1103/PhysRevB.75.012103 PACS number(s): 68.08.−p, 64.70.Dv, 81.30.Fb

At the high crystallization rates characteristic of rapid-solidification conditions, the magnitude and anisotropy of the interface mobility (μ), defined as the constant of proportionality between isothermal growth velocity and undercooling, can play a dominant role in governing the selection of growth morphologies and dendrite tip velocities, as demonstrated in recent phase-field simulations of rapid solidification in Ni.[1] Quantitative modeling of dendritic solidification under rapid-solidification conditions is hindered by the significant challenges associated with direct experimental measurements of μ and the associated lack of measured values available for this parameter.[2,3] In the absence of experimental data, the most detailed information underlying the current theoretical understanding of crystal-melt interface mobilities has been derived from atomic-scale molecular dynamics (MD) and Monte Carlo (MC) simulations.[4–21]

In 1986, Broughton, Gilmer, and Jackson presented the first MD simulation of isothermal crystallization in the Lennard-Jones (LJ) system.[4] Since this pioneering work, numerous computer-simulation studies of crystallization kinetics have been performed on a variety of elemental systems with fcc and bcc crystal structures.[4–21] These simulations have provided important insights into the atomic-scale processes underlying crystallization kinetics in systems with molecularly rough interfaces. Specifically, it was noted by Broughton, Gilmer, and Jackson, that crystallization kinetics for the pure LJ system is governed not by diffusive time scales, but rather by the frequency of adatom collisions with the crystal-growth surface. These results are consistent with observations of Turnbull and co-workers[22,23] who first referred to the crystallization kinetics of elemental metals as being "collision limited." Another important contribution from MD simulation studies was the discovery of an appreciable crystalline anisotropy in the interface mobility of elemental fcc-forming systems. For the LJ system, Burke *et al.* found that {100} is the fastest growth direction and the mobility for this orientation is two to three times larger than that corresponding to the {111} interface normals.[5] Comparable anisotropy in the interface mobility has been derived in more recent simulations for the low-index {100}, {110}, and {111} interfaces in the LJ system[11] as well as the fcc-forming metals Ni, Ag, Au, Cu, and fcc-Fe.[12,14,15,19,20] For each of these systems the fastest and slowest growth rates in MD are found for {100} and {111} interface orientations, respectively, and the calculated kinetic anisotropies span the range μ_{100}/μ_{110} around 1.4–1.8 and μ_{100}/μ_{111} around 2.0–3.6. Recently MD simulations have been extended in studies of crystallization kinetics for a few bcc-forming metals, where it was found that, relative to fcc-forming systems, the nature of the kinetic anisotropies are less universal and more dependent on the details of the interatomic potential. Specifically, Sun *et al.*[19] reported that the mobility anisotropy in bcc Fe is similar to that obtained by MD for fcc metals, namely $\mu_{100} > \mu_{110} > \mu_{111}$, while for molybdenum, Hoyt, Asta, and Sun[21] found that μ in the {110} direction is larger than that for {100} or {111}, whereas for vanadium calculated mobilities were isotropic within statistical uncertainty.[21]

Despite the significant technological interest in hexagonal metals such as Mg, Cd, and Zn, the properties of crystal-melt interface for systems which solidify into hexagonal-close-packed (hcp) crystal structures have been far less investigated. Specifically, we are unaware of any work to date reporting results for isothermal crystallization kinetics in hcp systems. In the present work we have undertaken a MD simulation study to compute the interface mobility of hcp Mg using a recently developed embedded-atom-method (EAM) interatomic potential.[24] In the remainder of this Brief Report we will summarize the computational details of our MD investigations, after which crystal-melt interface mobilities are presented and discussed in the context of previous MD results and theoretical models for the crystalline anisotropy of μ.

The simulation results presented in this report are based on an embedded-atom-method (EAM) interatomic potential for Mg published recently by Sun *et al.*[24] The potential was developed by fitting to experimentally measured and

first-principles-calculated properties for both crystalline and liquid bulk phases, as well as melting temperatures (T_M) for hcp and metastable-bcc solids. The potential thus represents an extension of earlier work by Liu *et al.* who developed an EAM potential for Mg employing the force-matching method.[25] Compared to this earlier potential, the one published by Sun *et al.* is selected for the present work since the EAM potential of Liu *et al.* was reported in Ref. 24 to give rise to an hcp-bcc transition upon heating at zero pressure, such that the coexistence between hcp Mg and the liquid phase at the hcp melting point is metastable. Such metastability can lead to potential artifacts in simulating melt coexistence and crystallization kinetics, and the EAM potential presented in Ref. 24 is preferred for the current work since it gives rise to stable coexistence between the hcp crystal and its melt. Another desirable feature of the potential in Ref. 24 is that, due to the use of the melting temperature in its fitting, the potential yields melting properties for hcp Mg in very reasonable agreement with experimental measurements. In particular, the equilibrium melting temperature, calculated by MD using a slight modification[20] of the coexistence approach introduced by Morris and co-workers,[26–28] was found to be just 9° below experiment.

Several methods have been proposed for calculating crystallization kinetics and interface mobilities from MD simulations, as reviewed in Refs. 20 and 16. In the present work, the so-called free solidification technique is employed. The approach involves measurements of steady-state interface velocities derived in isothermal simulations at constant pressure. Specifically, we make use of simulations employing NP_zAT dynamics, where the total number of atoms (N) is fixed, the cross-sectional area (A) of the simulation cell parallel to the interface is held constant, the length of the simulation cell perpendicular to the interfaces (L_z) is dynamic to give zero average normal stress,[31,32] and the temperature is held constant through the use of a Nosè-Hoover thermostat.[29,30] The equations of motion were integrated with a predictor-corrector algorithm with a time step of 0.002 ps.

To derive interface mobilities we compute the relationship between the steady-state interface velocity and the undercooling from MD simulations performed as above. For each undercooling, three separate solid-liquid starting configurations were generated from snapshots of solid-liquid coexistence simulations performed at the equilibirum melting point. To ensure uncorrelated initial states, the configurations were selected at 50-ps intervals and subsequently equilibrated for an additional 100 ps. The initial system contained 20% crystal (liquid) for the crystalizing (melting) runs. The total run time for each undercooling or orientation was around 0.6–1.2 ns. The interfacial mobility was calculated for three high-symmetry orientations of hcp Mg. In the standard four-index system for a hexagonal crystal, the three orientations studied were (0001), $(10\bar{1}0)$, and $(11\bar{2}0)$. For all the orientations, the simulation cell is built according to the lattice constant of the crystal at the melting temperature. The size parallel to the interface is about 30×30 Å for all orientations; these cross-sectional dimensions were chosen based on the zero-stress bulk lattice constant of the crystal, and were held fixed during the simulations to avoid stress in the crystal due to the interface. Each system contained roughly 10 000 atoms.

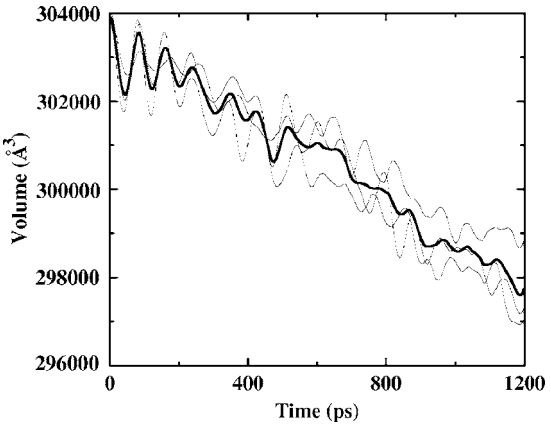

FIG. 1. The volume as a function of time during a free solidification simulation for a $(10\bar{1}0)$ oriented interface with 12 000 particles. The thin lines represent results from three independent runs, while the thick line is the average.

Figure 1 plots the volume of the MD simulation cell as a function of time, for a representative free-solidification simulation, performed at an undercooling of about 10 K for the (0001) orientation of the solid-liquid interface. As the system solidifies, the total volume of the simulation cell decreases due to the increasing volume-fraction of the higher-density solid phase. In the figure, the thin solid lines represent results derived from three independent starting configurations, and the solid line represents an average over the three runs. One can see that the system undergoes a transient behavior for an initial period of approximately 200 ps, before steady-state growth is established. The general behavior is consistent with results obtained in previous studies[19–21] on a variety of EAM systems. From the results plotted in Fig. 1, and a knowledge of the volume difference between bulk solid and liquid phases, the interface velocity V can be readily extracted.[20]

Figure 2 shows the crystal-melt-interface velocity (V) vs undercooling (overheating) for Mg, as determined from the free solidification MD simulations described above. Data for a total of six temperatures, three above and three below T_M, are plotted for each of the three growth directions (0001), $(10\bar{1}0)$, and $(11\bar{2}0)$. The open symbols represent the values of V averaged over the three independent runs for each undercooling. The error bars denote estimated uncertainties (standard statistical errors) in the mean value of V obtained from the variance of the interface velocities derived separately from each of the three independent simulations for a given temperature. The solid lines in Fig. 2 represent linear least-squares fits to the velocity-undercooling relations for each of the three orientations. In Fig. 2, one can see that the velocity-undercooling relations for the $(10\bar{1}0)$ and $(11\bar{2}0)$ orientations are nearly equivalent (within statistical uncertainties), while the velocities for the (0001) interface are clearly smaller in magnitude. For each orientation, the simulation data is modeled well by a linear relation between V

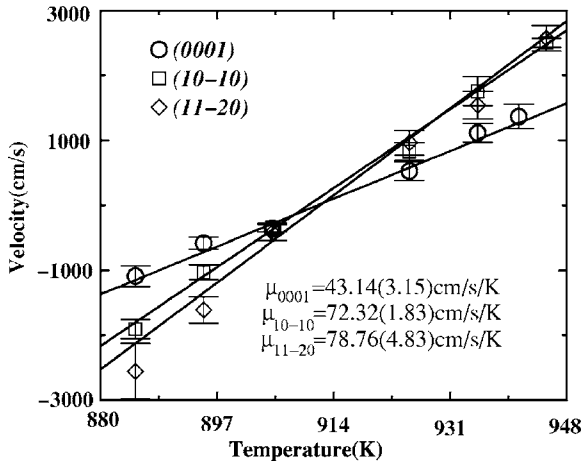

FIG. 2. Velocity of the crystal-melt interface vs temperature for Mg in the (0001), $(10\bar{1}0)$, and $(11\bar{2}0)$ directions. The solid lines are linear-least-squares fits to the data, the slopes of which yield the value of the interface mobility.

and undercooling. From the slopes of the least-squares-fitted lines, we obtain the values of μ listed in Table I.

As shown in Table I, an anisotropy of $\mu_{(10\bar{1}0)} \approx \mu_{(11\bar{2}0)} > \mu_{(0001)}$ for hcp Mg is obtained in the present work. Since fcc and hcp share many similarities in their structure, it is interesting to compare the anisotropy in mobility for an hcp crystal with that of fcc. First, the in-plane structure and atomic density of hcp (0001) is the same as that for fcc (111), and both orientations have similar layer spacing. Interestingly, both hcp (0001) and fcc (111) have the smallest μ compared with other high symmetry orientations. Similarly, the in-plane atomic structure of hcp $(10\bar{1}0)$ is qualitatively comparable to fcc (110) and the ratio $\mu_{10\bar{1}0}/\mu_{0001}$ for hcp Mg is about 1.7 from the current calculations, which is very similar to the value of μ_{110}/μ_{111} in a fcc system (about 1.4–2.0 for different systems). The similarity between the hcp and fcc anisotropy implies a strong correlation between μ and interface structure, a correlation which is also reflected in Mikheev-Chernov model for μ,[33,34] as discussed below.

In 1991, Mikheev and Chernov developed a kinetic density-functional theory for isothermal crystallization rates in systems with molecularly rough solid-liquid interfaces.[33,34] Previous MD calculations for fcc-based systems have yielded mobility anisotropies which are comparable to those predicted by the Mikheev-Chernov model, as discussed in Refs. 19 and 20. Here we will examine the nature of the anisotropies of μ derived by MD for Mg by extending the Mikheev-Chernov model to the hcp case.

To derive an analytical expression for μ, Mikheev-Chernov expressed the number density in a heterogeneous solid-liquid system in terms of "density waves," i.e., Fourier density modes constructed from the reciprocal-lattice vectors of the underlying crystal, with amplitudes that vary spatially across the interface. Isothermal crystallization velocities are then derived by considering the growth rates of the amplitudes of these Fourier modes. The resulting MC expression for the kinetic coefficient is given by

$$\mu = \frac{L}{k_B T_m^2} \frac{S(G_1)\xi_b}{\tau(G_1)\sum_{N_1} 1/\cos(\theta)}, \tag{1}$$

where $S(k)$ is the liquid structure factor and $k=G_1$ refers to the first main peak position. The bulk correlation length in the liquid, ξ_b, is given as the inverse half width of the main peak in $S(k)$. The relaxation time for density fluctuations in the bulk liquid is denoted by τ. Anisotropy in the Mikheev-Chernov model is reflected in the summation term appearing in Eq. (1). The sum extends over the N_1 (equal to 8 for fcc) first-neighbor reciprocal-lattice vectors and θ is the angle between the reciprocal-lattice vector and the normal to the solid-liquid interface.

To apply the Mikheev-Chernov model to the case of Mg, we note that the hcp crystal structure can be constructed from reciprocal-lattice vectors corresponding to the underlying hexagonal Bravais lattice. Specifically, if we take as the translational vectors of the hcp structure:

$$\vec{a}_1 = \left(-\frac{a}{2}, -\frac{\sqrt{3}a}{2}, 0\right); \quad \vec{a}_2 = (a,0,0); \quad \vec{a}_3 = (0,0,c)$$

then the corresponding reciprocal-lattice vectors are

$$\vec{b}_1 = \left(0, -\frac{2}{\sqrt{3}a}, 0\right); \quad \vec{b}_2 = \left(\frac{1}{a}, -\frac{1}{\sqrt{3}a}, 0\right); \quad \vec{b}_3 = \left(0,0,\frac{1}{c}\right).$$

The Fourier representation of an hcp crystal structure contains modes with nonzero amplitudes only for those wave vectors which are linear combinations of the above reciprocal-lattice vectors. In the Mikheev-Chernov model, it is assumed that of all the (formally infinite in number) Fourier modes required to construct the time-averaged density in the crystal, only those with the shortest wave vectors contribute significantly to the interface mobility, since these modes with k nearest to G_1 have the longest relaxation times in the bulk liquid. Applying the same reasoning to the case of the hcp crystal structure, it is reasonable to assume that the motion of the interface will be dominated by the growth rates of the Fourier modes with wave vectors having magnitudes lying closest to the first peak in the liquid structure factor. For hcp there are then six wave vectors to consider in the Mikheev-Chernov model, namely $\mathbf{G}=(0,1,0)$; $(0,-1,0)$; $\left(\frac{\sqrt{3}}{2},-\frac{1}{2},0\right)$; $\left(-\frac{\sqrt{3}}{2},\frac{1}{2},0\right)$; $\left(-\frac{\sqrt{3}}{2},-\frac{1}{2},0\right)$; $\left(\frac{\sqrt{3}}{2},\frac{1}{2},0\right)$, in units of $2/\sqrt{3}a$. By considering these six G vectors in performing the sum in the denominator of Eq. (1), we obtain the following predictions for the kinetic anisotropy for a hcp crystal-melt interface: $\mu_{10\bar{1}0}/\mu_{0001}=1.90$ and $\mu_{11\bar{2}0}/\mu_{0001}=1.73$. The analysis thus predicts μ_{0001} to be the smallest in magnitude, while $\mu_{10\bar{1}0}$ and $\mu_{11\bar{2}0}$ are comparable, in agreement with the MD results for Mg. Further, the Mikheev-Chernov-model

TABLE I. The interfacial mobility (μ) in units of cm/s/K for hcp Mg in the low-index growth directions (0001), $(11\bar{2}0)$, and $(10\bar{1}0)$. Error bars denote estimated 95% confidence intervals.

μ_{0001}	$\mu_{10\bar{1}0}$	$\mu_{11\bar{2}0}$
43.14±3.15	71.32±1.83	78.76±4.83

predictions for the magnitude of the anisotropy in μ between the close-packed {0001} direction relative to the more open $\{10\bar{1}0\}$ and $\{11\bar{2}0\}$ orientations are in very reasonable quantitative agreement with the MD results yielding $\mu_{10\bar{1}0}/\mu_{0001} = 1.65 \pm 0.13$ and $\mu_{11\bar{2}0}/\mu_{0001} = 1.83 \pm 0.17$. It is also of interest to compare the magnitude of μ for the hcp(0001) to that of fcc(111), that is, the two close-packed directions. The Mikheev-Chernov model predicts a ratio of growth rates as

$$\frac{\mu^{fcc}}{\mu^{hcp}} = \frac{L^{fcc}(T_m^{hcp})^{3/2} A_s^{hcp}}{L^{hcp}(T_m^{fcc})^{3/2} A_s^{fcc}}, \tag{2}$$

where A_s, the anisotropy factor, is given by the summation in Eq. (1). Using the result for fcc Ni[20] and the present result for Mg (0001), we find a ratio of 0.68 which is comparable to, but roughly 20% higher, than the MD value of 0.56. The level of agreement between the Mikheev-Chernov model and the MD results obtained in this work for Mg suggests that the nature and magnitude of the anisotropies in hcp systems may be associated with the crystal structure, as has been found in previous MD studies of fcc-based systems.

In summary, we have presented MD simulations of crystal-melt interface mobilities in hcp Mg for three high symmetry orientations (0001), $(10\bar{1}0)$, and $(11\bar{2}0)$. The results show that the $\mu_{(10\bar{1}0)}$ and $\mu_{(11\bar{2}0)}$ are very close in magnitude, while μ_{0001} is about 1.7 times smaller relative to the other two orientations. Interestingly, for both fcc and hcp systems, the close-packed surfaces, namely fcc(111) and hcp(0001), have the lowest growth rate. In addition, the kinetic DFT model of Mikheev and Chernov was extended to the case of hcp crystals and it was found that the kinetic anisotropies can be semiquantitatively predicted by the model.

This research was supported by the National Science Foundation of China, the Shanghai Municipal Education Commission and Shanghai Education Development Foundation, and the Scientific Research Foundation for the Returned Overseas Chinese Scholars, State Education Ministry (Z.G.X. and D.Y.S.). M.A. and J.J.H. acknowledge support from US-DOE Contract No. DOE-FG02-06ER46282 and the DOE Computational Materials Science Network (CMSN) program. Use was made of resources at the National Energy Research Scientific Computing Center, which is supported by the Office of Science of the DOE under contract DE-AC03–76SF00098.

[1] J. Bragard, A. Karma, Y. H. Lee, and M. Plapp, Interface Sci. **10**, 121 (2002).
[2] M. E. Glicksman and R. J. Schaefer, J. Cryst. Growth **1**, 297 (1967).
[3] G. H. Rodway and J. D. Hunt, J. Cryst. Growth **112**, 554 (1991).
[4] J. Q. Broughton, G. H. Gilmer, and K. A. Jackson, Phys. Rev. Lett. **49**, 1496 (1982).
[5] E. Burke, J. Q. Broughton, and G. H. Gilmer, J. Chem. Phys. **89**, 1030 (1988).
[6] C. J. Tymczak and J. R. Ray, Phys. Rev. Lett. **64**, 1278 (1990); J. Chem. Phys. **92**, 7520 (1990).
[7] C. F. Richardson and P. Clancy, Mol. Simul. **7**, 335 (1991); Phys. Rev. B **45**, 12260 (1992).
[8] R. Moss and P. Harrowell, J. Chem. Phys. **100**, 7630 (1994).
[9] W. J. Briels and H. L. Tepper, Phys. Rev. Lett. **79**, 5074 (1997).
[10] H. E. A. Huitema, M. J. Vlot, and J. P. van der Eerden, J. Chem. Phys. **111**, 4714 (1999).
[11] H. E. A. Huitema, B. van Hengstum, and J. P. van der Eerden, J. Chem. Phys. **111**, 10248 (1999).
[12] J. J. Hoyt, B. Sadigh, M. Asta, and S. M. Foiles, Acta Mater. **47**, 3181 (1999).
[13] H. L. Tepper and W. J. Briels, J. Cryst. Growth **230**, 270 (2001); J. Chem. Phys. **115**, 9434 (2001); **116**, 5186 (2002).
[14] F. Celestini and J.-M. Debierre, Phys. Rev. E **65**, 041605 (2002).
[15] J. J. Hoyt and M. Asta, Phys. Rev. B **65**, 214106 (2002).
[16] J. J. Hoyt, M. Asta, and A. Karma, Interface Sci. **10**, 181 (2002).
[17] K. A. Jackson, Interface Sci. **10**, 159 (2002).
[18] J. J. Hoyt, M. Asta, and A. Karma, Mater. Sci. Eng., R. **41**, 121 (2003).
[19] D. Y. Sun, M. Asta, and J. J. Hoyt, Phys. Rev. B **69**, 174103 (2004).
[20] D. Y. Sun, M. Asta, and J. J. Hoyt, Phys. Rev. B **69**, 024108 (2004).
[21] J. J. Hoyt, M. Asta, and D. Y. Sun, Philos. Mag. **86**, 3651 (2006).
[22] D. Turnbull and B. G. Bagley, Solid State Chem. **5**, 526 (1975).
[23] S. R. Coriell and D. Turnbull, Acta Metall. **30**, 2135 (1982).
[24] D. Y. Sun, M. I. Mendelev, C. A. Becker, K. Kudin, T. Haxhimali, M. Asta, J. J. Hoyt, A. Karma, and D. J. Srolovitz, Phys. Rev. B **73**, 024116 (2006).
[25] X.-Y. Liu, J. B. Adams, F. Ercolessi, and J. A. Moriarty, Modell. Simul. Mater. Sci. Eng. **4**, 293 (1996).
[26] J. R. Morris, C. Z. Wang, K. M. Ho, and C. T. Chan, Phys. Rev. B **49**, 3109 (1994).
[27] J. R. Morris and X. Y. Song, J. Chem. Phys. **116**, 9352 (2002).
[28] M. P. Allen and D. J. Tildesley, *Computer Simulation of Liquids* (Clarendon, Oxford, 1993).
[29] S. Noše, J. Chem. Phys. **81**, 511 (1984); Mol. Phys. **52**, 255 (1984).
[30] W. G. Hoover, Phys. Rev. A **31**, 1695 (1985); **34**, 2499 (1986).
[31] H. C. Andersen, J. Chem. Phys. **72**, 2384 (1980).
[32] M. Parrinello and A. Rahman, Phys. Rev. Lett. **45**, 1196 (1980); J. Appl. Phys. **52**, 7182 (1981); J. Chem. Phys. **76**, 2662 (1982).
[33] L. V. Mikheev and A. A. Chernov, J. Cryst. Growth **112**, 591 (1991).
[34] L. V. Mikheev and A. A. Chernov, Sov. Phys. JETP **65**, 971 (1987).